



Late Holocene hydroclimate variability and human–environment interactions in the Cuenca Oriental, Mexico: multiproxy evidence from Lake Alchichica

Reza Safaierad ^{a,*¹}, Isabel Israde-Alcántara ^b, Marttiina Rantala ^{a,c}, Gabriela Domínguez-Vázquez ^d, Mahyar Mohtadi ^e, Enno Schefuß ^e, Wojciech Tylmann ^f, Pierre Francus ^g, Nadine Mattielli ^c, Sarah Metcalfe ^h, Nathalie Fagel ^a

^a Argiles, Géochimie et Environnement sédimentaires (AGEs), Université de Liège, Liège, Belgium

^b Instituto de Investigaciones en Ciencias de la Tierra, Universidad Michoacana de San Nicolás de Hidalgo, Morelia, Mexico

^c Laboratoire G-Time, Université libre de Bruxelles, ULB, Brussels, Belgium

^d Facultad de Biología, Universidad Michoacana de San Nicolás de Hidalgo, Morelia, Mexico

^e MARUM-Center for Marine Environmental Sciences, University of Bremen, Bremen, Germany

^f Department of Geomorphology and Quaternary Geology, University of Gdańsk, Gdańsk, Poland

^g Centre Eau Terre Environnement, Institut national de la recherche scientifique, Québec City, Canada

^h School of Geography, University of Nottingham, Nottingham, United Kingdom

ARTICLE INFO

Handling Editor: Dr P Rioual

Keywords:

Hydroclimate
Lacustrine sediment
Late classic drought
Anthropogenic activity
Geochemistry
Maize

ABSTRACT

The Cuenca Oriental, a semi-arid region in east-central Mexico, has long supported complex societies, yet its hydroclimatic variability and human–environment interactions—particularly during the Classic, Postclassic, and Colonial periods—remain poorly understood. Here, we present high-resolution proxy records from Lake Alchichica, a crater lake located 18 km from the ancient city of Cantona (600–1050 CE), to reconstruct environmental conditions in the Cuenca Oriental over the past five millennia. Isotope records reveal three major dry periods: (I) ca. 500–1300 CE, encompassing and extending beyond the Late Classic Drought (770–1100 CE); (II) the 17th century CE, corresponding to a colder phase of the Little Ice Age; and (III) post-1970 CE, coinciding with the peak of ongoing global warming. Anthropogenic indicators—including maize and other anthropogenic pollen, as well as *Glomus* spores and titanium (Ti) intensity (proxies for soil erosion)—demonstrate sustained human–environment interactions. Maize cultivation began by the mid-first millennium BCE and peaked during the Postclassic period (ca. 1000–1500 CE), followed by a sharp and prolonged decline after the Spanish Conquest, most likely due to demographic collapse driven by the introduction of Old World diseases. Agricultural activity never returned to Postclassic maxima, marking a lasting transformation in land use and food production. Notably, the entire urban lifespan of Cantona was encompassed by the extended drought period (500–1300 CE), and its collapse occurred under climatic conditions comparable to those during its peak. Furthermore, the concurrent intensification of agriculture near Lake Alchichica and the abandonment of Cantona suggest that climate alone does not fully explain the decline of the city, instead pointing to additional factors such as warfare, socio-political instability, and economic disruption.

1. Introduction

Mexico, as part of Mesoamerica, has a long-standing history of human–environment interactions during the Holocene (Leyden, 1987; Matsuoka et al., 2002; Metcalfe et al., 1989; Piperno and Flannery,

2001). Climatically, Mexico is influenced by several atmospheric circulation systems. In much of northern and central Mexico, the primary source of summer precipitation is the North American Monsoon (also known as the Mexican Monsoon) (Adams and Comrie, 1997). Meanwhile, precipitation patterns in southern Mexico are more strongly

* Corresponding author.

E-mail address: Safaierad.reza@gmail.com (R. Safaierad).

¹ Present address: Department of Geography, Institute for Integrated Natural Sciences, University of Koblenz, Koblenz, Germany.

influenced by the Intertropical Convergence Zone (ITCZ) and its associated variations in the tropical easterlies, including the Trade Winds and easterly waves. Within this climatic framework, hydroclimate variability has likely played a critical role in shaping patterns of human activity and landscape transformation over the Holocene (Curtis et al., 1996; Haug et al., 2003; Hodell et al., 1995). Moreover, climate model projections indicate that Mexico and much of Mesoamerica are likely to face increased drying in the future (Colorado-Ruiz et al., 2018; Knutti and Sedláček, 2013), underscoring the importance of understanding how past societies responded to drought and hydroclimatic stress. Yet, the precise nature of the relationship between past climatic fluctuations and human–environment dynamics remains poorly understood.

Studies addressing land-use change and landscape management have been undertaken in both the tropical lowlands (Brenner et al., 2002; Estrada-Belli and Wahl, 2010; Goman et al., 2010; Turner and Sabloff, 2012; Wahl et al., 2013; Walsh et al., 2014) and the highlands of Mexico (Almeida-Leñero et al., 2005; Arnauld et al., 1997; Bhattacharya and Byrne, 2016; Bhattacharya et al., 2015; Metcalfe and Davies, 2007; Metcalfe et al., 2010; Ortega-Guerrero et al., 2021; Park et al., 2010; Vázquez et al., 2010). Despite these efforts, considerable uncertainty persists regarding the scale and intensity of anthropogenic activity during the Late Holocene, particularly during the Formative, Classic, Postclassic, and Colonial (or Historic) periods. One key area of debate concerns whether human impact on the landscape intensified more markedly before or after the Columbian encounter (1521 CE). Research conducted in the Mexican highlands has yielded divergent conclusions. While some studies suggest a significant increase in anthropogenic activity during the post-Columbian era (Bhattacharya and Byrne, 2016; Elliott et al., 2010; Fisher, 2005; Gerez-Fernández, 1985; Simpson, 1952), others indicate that land-use changes following the Spanish conquest were relatively modest (Butzer and Butzer, 1997). These discrepancies suggest the heterogeneous nature of regional responses to colonial processes. As such, further interdisciplinary and regionally nuanced research is required to deepen our understanding of the complex dynamics of human activity in relation to environmental change across different parts of Mexico.

The Cuenca Oriental in east-central Mexico is a region of substantial paleoenvironmental and archaeological importance, particularly for understanding human–environment interactions during the Holocene. Its volcanic landscapes, closed-basin lakes, and fertile plains made it a compelling setting for early human settlement and transformation. This region served as a major cultural and economic center during the Pre-classic (c.1800 BCE–250 CE), Classic (c.250–900 CE), and Postclassic (c.900–1521 CE) periods. It was home to Cantona (600–1050 CE), one of the largest cities in pre-Columbian Mesoamerica, located in present-day Puebla. Cantona's prominence stemmed from its proximity to the Oyameles-Zaragoza obsidian mines and its strategic position along trade routes linking the Gulf of Mexico with the central highlands (García-Cook and Merino, 1998; Knight and Glascock, 2009). At its peak around 700 CE, it supported an estimated population of 90,000 (García-Cook and Merino, 1998). Although Cantona's occupation began in the Preclassic (600 BCE–250 CE), its third (600–900 CE) and fourth (900–1050 CE) cultural phases are most notable—the former marked by urban prosperity and walled infrastructure (García Santos et al., 2012), and the latter by population decline and eventual abandonment (García-Cook and Merino, 1998; García Santos et al., 2012). While persistent arid conditions prevailed throughout its urban history, climate change has been suggested as a contributing factor in its decline (Bhattacharya et al., 2015). Nonetheless, the paleoclimate history of the region remains poorly characterized, and evidence of human–environment interactions is still limited. In particular, our

understanding of climatic variability during the Late Holocene is fragmentary, and the extent and intensity of anthropogenic activities during different cultural periods remain insufficiently documented. While a few studies have provided preliminary insights into hydroclimate changes (Bhattacharya and Byrne, 2016; Bhattacharya et al., 2015; Caballero et al., 2003), the relationship between these environmental shifts and human activity is not yet well understood.

In this study, we present proxy records spanning the past five millennia, derived from a lacustrine sediment core obtained from Lake Alchichica, a maar lake located in the Cuenca Oriental of Mexico, approximately 18 km southeast of the ancient city of Cantona (Fig. 1B). Our dataset integrates geochemical (including elemental and stable isotope analyses), palynological, and mineralogical proxies to provide independent lines of evidence for past hydroclimate variability and human activity. We reconstruct hydroclimate conditions and put them within a broader regional framework to enhance understanding of long-term climate variability in the Cuenca Oriental. Furthermore, we identify signatures of past anthropogenic activities, including maize cultivation and related land-use changes such as erosion likely driven by human disturbance in the Lake Alchichica catchment. Finally, we explore the relationship between climate variability and cultural dynamics from the Classic period onward, positioning Lake Alchichica as a key site for understanding socio-environmental change in the Cuenca Oriental. The proximity of Lake Alchichica to Cantona provides a record that is geographically more relevant to the city than previous paleoenvironmental reconstructions. This makes Alchichica a particularly valuable archive for linking regional hydroclimate variability with the settlement history of Cantona.

2. Regional setting (the lake, climate and vegetation)

Located in the eastern sector of the Trans-Mexican Volcanic Belt (TMVB), Lake Alchichica is the deepest maar lake in Mexico, reaching a depth of 66 m (Fig. 1C) (Kaźmierzak et al., 2011). It is a closed basin system (Silva-Aguilera et al., 2025), primarily recharged by precipitation and groundwater. Evaporation serves as the main pathway for water loss, leading to a persistently negative water balance (Alcocer et al., 2004). This hydrological regime contributes to the lake's alkaline ($\text{pH} > 9$) and moderately saline (8.5 g/L) conditions (Caballero et al., 2003). Lake Alchichica is a warm monomictic, oligotrophic lake exposed to high solar radiation, which promotes microbial photosynthesis and the precipitation of calcium carbonate. Consequently, extensive carbonate microbialites (stromatolites) have developed along its shores (Tavera and Komárek, 1996), making the lake a valuable modern analog for studying early Earth environments.

The Cuenca Oriental exhibits a semi-arid to temperate highland climate, characterized by moderate temperatures resulting from its elevation (~2300 m a.s.l.), a marked seasonality in precipitation (Fig. 1D), and high evaporation rates. Long-term data from the Alchichica meteorological station indicate an average annual evaporation of 1900 mm, significantly exceeding the mean annual precipitation of 390 mm. Rainfall is primarily concentrated between May and October, driven by the Mexican monsoon (Higgins et al., 1997). Notably, the region experiences a mid-summer minimum in precipitation known as the canícula (Magaña et al., 1999), as illustrated in Fig. 1D. This interruption, which can persist for several weeks, is particularly important due to its potential impacts on soil moisture, crop productivity, and overall agricultural practices in the region. The semi-arid climatic regime of the Cuenca Oriental contributes to the development of alkaline and saline conditions in the region's endorheic lakes, such as Lake Alchichica, and plays a fundamental role in shaping their

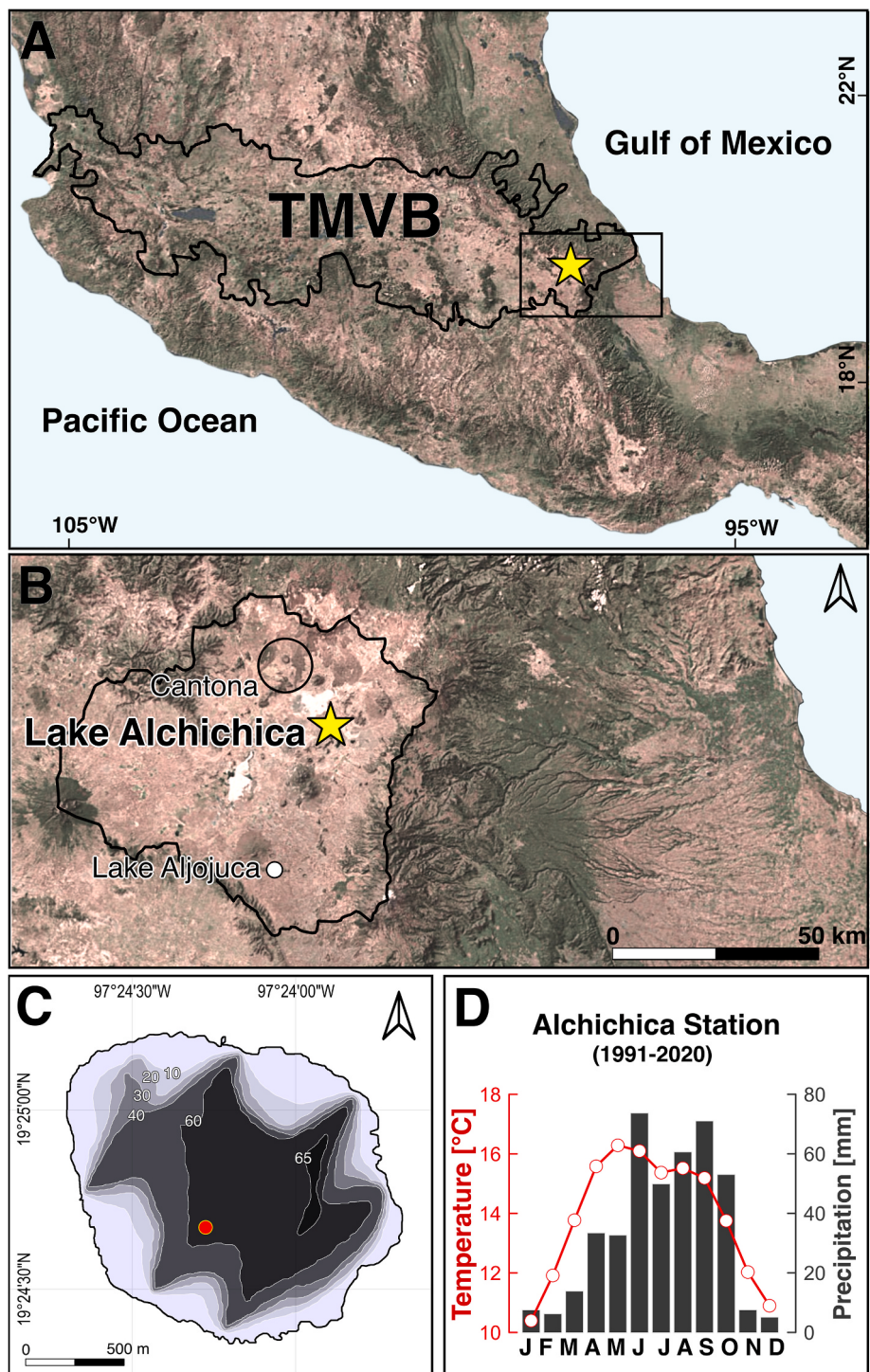


Fig. 1. Location of the study area in eastern Mexico. (A) Lake Alchichica (yellow star) is situated in the eastern sector of the Trans-Mexican Volcanic Belt (TMVB). The black rectangle marks the area shown in map (B). (B) Detailed view of the Cuenca Oriental, showing the locations of Cantona (black circle), Lake Alchichica (yellow star), and Lake Aljojuca (white circle). The background aerial photographs are obtained from <https://satellites.pro>. (C) Bathymetric map of Lake Alchichica. The red circle marks the location of the coring site. The map is modified from Arredondo-Figueroa et al. (1983). (D) Climate diagram showing 30-year (1991–2020 CE) mean monthly temperature and precipitation near Lake Alchichica. (For interpretation of the references to colour in this figure legend, the reader is referred to the Web version of this article.)

distinctive geochemical and ecological characteristics.

Due to the semi-arid climate and the leeward position of the Cuenca Oriental, the local vegetation primarily consists of scrublands interspersed with scattered trees. In the highlands of the Cuenca Oriental, oak forests, dominated by various *Quercus* (oak) species, are prevalent (Ernesto Rivera-Hernandez et al., 2019). Further east, about 20 km from the lake, humid temperate pine-oak forests thrive on the windward slopes. Beyond the natural vegetation, the land around the lake is used for cereal cultivation, with maize being the dominant crop.

3. Materials and methods

3.1. Sediment coring and radiometric dating

In April 2022, a 57-cm-long lacustrine core was collected from Lake Alchichica ($19^{\circ} 24' 38''$ N, $97^{\circ} 24' 14''$ W, 2322 masl) at a water depth of ~60 m (Fig. 1C) using a Uwitec® coring device equipped with a 9-cm coring tube. The core was split lengthwise, analyzed using core scanning techniques, and subsampled.

To establish a chronology for the sediment core, dating methods included radiolead (^{210}Pb) for the younger sediments and radiocarbon (^{14}C) for the sections extending beyond the range of ^{210}Pb applicability. For ^{210}Pb dating, 20 freeze-dried subsamples of 0.2 g from the upper 20 cm of the core were analyzed with alpha spectrometry at the University of Gdańsk, Poland, according to procedures presented in Tylmann et al. (2016).

Obtaining reliable ^{14}C dates for sediments in carbonate basins, such as Lake Alchichica, is particularly challenging due to the potential influence of old carbon in the lake water. Incorporating old carbon by organisms living in the lake can result in inaccurate radiocarbon ages, making the sediments that host these organisms appear older than their true age (e.g., Jull et al., 2013; Stuiver and Östlund, 1983). To address this potential issue, we used pollen extracts for radiocarbon dating. Pollen grains were extracted and concentrated from ~25 g of wet sediment following the procedure outlined by Tunno et al. (2021), which involved treatment with 10 % KOH, 3N HCl, removal of coarse ($>80 \mu\text{m}$) and fine fractions ($<30 \mu\text{m}$), elimination of organic matter using 2.5 % NaOCl, and pollen flotation with sodium polytungstate (1.9 specific gravity). The pollen extracts were submitted for radiocarbon dating to the Center for Science and Education Radiocarbon and Mass Spectrometry Laboratory at the Institute of Physics, Silesian University of Technology, Poland. Radiocarbon dates were calibrated using the Northern Hemisphere terrestrial calibration curve IntCal20 (Reimer et al., 2020), and an age-depth model was created in RStudio v4.4.1 (Team, 2020) using the *rplum* v0.5.1 package (Aquino-López et al., 2018), combining ^{210}Pb and ^{14}C data.

3.2. Sediment core scanning

Geochemical compositions of the sediment core were analyzed using an ITRAX X-ray fluorescence core scanner (CS-XRF) at the INRS Centre Eau Terre Environnement (Québec City, Canada). The analysis produced the ratio of Compton (incoherent) to Rayleigh (coherent) scattering (Inc/Coh), which can serve as an indicator of sediment organic content (Woodward and Gadd, 2019). The scans were measured at 2 mm intervals using 20 kV with a current of 10 mA and a dwell time of 20 s. To reduce matrix effects and address the closed-sum issue, elemental intensities measured in counts per second were transformed using the centered log-ratio (clr) method (Weltje et al., 2015). For better visualization, all elemental data were subjected to min-max normalization.

The core structure was revealed by a Siemens Somatom Definition +128 CT-scanner at the INRS Centre Eau Terre Environnement with a 0.31 mm resolution in the stratigraphic direction. Grey levels are expressed in Hounsfield units (HU): light (dark) grey levels represent dense (light) sediments.

3.3. X-ray diffraction mineralogy

Forty freeze-dried ground samples weighing ~0.5 g were sieved through a 150 μm mesh and transferred to a plastic holder using the backside method (Moore and Reynolds, 1989) and scanned from 2 to 70° 20 with a step size of 0.009° 20 and 0.5 s per step. The analysis was performed using a Bruker® D8-Advance Eco diffractometer (CuK α radiation, $\lambda = 1.5418 \text{ \AA}$, 40 kV, 25 mA) coupled with a Lynxeye XE detector (AGEs Laboratory, University of Liège, Belgium). Mineral identification and quantification were done using the EVA (v4.3) and TOPAS (v5.0) ® Bruker software, respectively (Fig. S2). A Rietveld refinement was applied to all the minerals identified by X-ray diffraction (XRD) (Rietveld, 1967; Środoń, 2002). Unit cell parameters and preferred orientations of the mineral phases were adjusted to obtain a reconstructed XRD pattern as close to the measured pattern.

3.4. Pollen analysis

A total of 39 wet sediment samples, each measuring 1 cm^3 , were used for pollen analysis. Pollen extraction was carried out at the Department of Geology, University of Liège, following the standard procedure (Faegri and Iversen, 1989), which involved treatments with 10 % HCl, 37 % HF, acetolysis and sieving through a 10 μm screen. Pollen samples were counted under $\times 400$ magnification using a Zeiss microscope, with a minimum of 300 terrestrial pollen grains counted per sample. Pollen from local aquatic plants (e.g., Cyperaceae) and non-pollen palynomorphs, including fungal remains (e.g., *Glomus* spores), were excluded from the total pollen sum. The pollen diagram and the dendrogram, developed using the constrained incremental sum of squares (CONISS) method, were plotted using the TILIA software (Grimm, 1987, 1991).

3.5. Bulk sediment oxygen isotope analysis

Samples were collected at 1 cm intervals and analyzed at MARUM-Center for Marine Environmental Sciences, University of Bremen (Germany), using a Finnigan MAT252 gas isotope ratio mass spectrometer coupled with a Kiel III automated carbonate preparation device. The results are presented in the standard delta notation (δ) relative to VPDB (Vienna Pee Dee Belemnite). The instrument was calibrated using a house standard (ground Solnhofen limestone), which was itself calibrated against the NBS 19 calcite reference. During the measurement period, the standard deviations for the house standard were 0.06 ‰.

3.6. Extraction and separation of leaf-wax n-alkanes

Leaf-wax n-alkanes were extracted from 20 dried and homogenized samples (weighing between 1.3 and 2.8 g dry weight) using a mixture of dichloromethane and methanol (DCM; 9:1 v/v) in a DIONEX Accelerated Solvent Extractor (Dionex ASE-200) at 100 °C and 1000 psi for 5 min, repeated three times. A known quantity of squalane was added as an internal standard before extraction. The total lipid extracts were concentrated using a rotary evaporator under N_2 flow until nearly dry and treated with activated copper (2N HCl) to remove elemental sulfur.

The extracts were then saponified with 0.5 mL of 6 % KOH in MeOH at 80 °C for 2 h. Neutral compounds such as hydrocarbons, ketones, and alcohols were extracted with hexane. Non-polar hydrocarbons were isolated via column chromatography using silica gel and hexane, followed by a silver nitrate-silica column to eliminate unsaturated compounds. The saturated hydrocarbon fractions were analyzed using Gas Chromatography with a Flame Ionization Detector (GC/FID) at MARUM, Center for Marine Environmental Sciences, University of Bremen. Individual *n*-alkanes were identified by comparing retention times with an external standard, and quantification precision was determined to be <5 % based on repeated measurements of the external alkane standard.

Hydrogen isotope analyses of *n*-alkanes were performed on a Thermo Fisher Scientific MAT 253 Isotope Ratio Mass Spectrometer coupled to a GC IsoLink operated at 1420 °C, connected to a Thermo Fisher Scientific TRACE GC equipped with an HP-5ms column (30 m, 0.25 mm, 1 µm). Each sample was analyzed in duplicate, with δD values calibrated against a reference H₂ gas of known isotopic composition and reported in ‰ VSMOW (Vienna Standard Mean Ocean Water). Accuracy and precision were verified using an internal *n*-alkane standard calibrated against the A4-Mix isotope standard (A. Schimmelmann, University of Indiana, USA) every six measurements, as well as by daily H₃⁺ factor determination. Long-term analytical precision was <3 ‰, with H₃⁺ factors ranging from 5.1 to 5.2. The squalane internal standard showed accuracy and precision of 3 ‰, while replicate analyses of the *n*-C₃₃ alkane yielded an average precision of 1 ‰.

Stable carbon isotope (δ¹³C) analyses of *n*-alkanes were conducted on a Finnigan MAT 252 Isotope Ratio Mass Spectrometer coupled via a GC/C interface with a combustion reactor operated at 1000 °C to a Thermo Fisher Scientific TRACE GC equipped with a HP-5ms column (30 m, 0.25 mm, 0.5 µm). Each sample was measured at least in duplicate and δ¹³C values calibrated against ‰ VPDB (Vienna PeeDee Belemnite). The long-term mean absolute deviation based on the external *n*-alkane standard mixture was 0.3 ‰ VPDB. The precision and accuracy of the squalane internal standard were 0.2 and 0.1 ‰ VPDB, respectively. The average reproducibility of δ¹³C analyses for the *n*-C₃₃ alkane was 0.1 ‰ VPDB. Instrument drift during leaf wax isotope measurements was negligible. System performance was routinely monitored by analyzing an external alkane standard mix every six runs. Analyses were paused if any compound showed a deviation greater than 3 ‰, and measurements were only resumed once values returned within accepted limits.

To assess the relative contributions of aquatic versus terrestrial plants to the sedimentary *n*-alkanes, we calculated the Paq index (Ficken et al., 2000) as follows:

$$\text{Paq} = \frac{n\text{C}23 + n\text{C}25}{n\text{C}23 + n\text{C}25 + n\text{C}29 + n\text{C}31}$$

where short-to mid-chain homologues (*n*-C₂₃, *n*-C₂₅) are characteristic of submerged and emergent aquatic macrophytes, while long-chain homologues (*n*-C₂₉, *n*-C₃₁) are typical of terrestrial higher plants. Values close to 0 indicate dominance of terrestrial plant input, while values approaching 1 suggest a strong aquatic contribution.

Additionally, to better capture the integrated hydrogen isotopic signal of terrestrial leaf waxes, we calculated the amount-weighted δD of long-chain homologues (*n*-C₂₉, *n*-C₃₁, *n*-C₃₃) following common practice in compound-specific isotope studies (e.g., Sachse et al., 2012). The δD_{weighted} is calculated as:

$$\delta D_{\text{weighted}} = \frac{\sum_i (\delta D_i * f_i)}{\sum_i f_i}$$

where δD_i represents the hydrogen isotopic composition (‰) of each homologue, and f_i is its relative abundance. This approach minimizes bias from any single homologue when values change in parallel and provides a more robust representation of the overall isotopic composition of plant waxes from the entire ecosystem.

4. Results and interpretation

4.1. Chronology and lithology

The Bayesian age-depth model based on ²¹⁰Pb data and three ¹⁴C dates indicates that the core spans the past five millennia (Fig. 2, Table 1 and Table S1). A distinct shift in sedimentation rate occurs at approximately 27 cm, increasing from an average of ~0.07 mm a⁻¹ in the lower section to ~0.33 mm a⁻¹ in the upper section. This change coincides with a lithological change from less dense to denser sediments, as indicated by a rise in mean grey values from 225 to 350 HU (Fig. 3). Additionally, the change in density follows an inverse pattern to the sediment organic content inferred from the inc/coh ratio (Fig. 3).

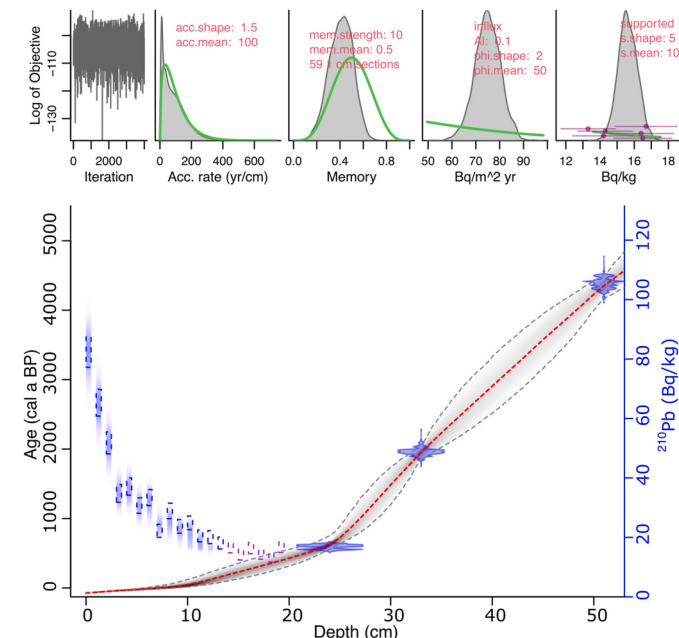


Fig. 2. Bayesian age-depth model for the Lake Alchichica sediment core. The age-depth model is developed using ²¹⁰Pb and ¹⁴C measurements. The main panel depicts the mean age estimates (red line) with 95 % confidence intervals (grey envelopes), along with total ²¹⁰Pb values (blue) and supported ²¹⁰Pb values (purple). The distribution of ¹⁴C ages is shown in blue (below 20 cm core depth). The upper panel illustrates the Markov Chain Monte Carlo (MCMC) iterations and the Bayesian parameter distributions, with priors in green and posteriors in grey. (For interpretation of the references to colour in this figure legend, the reader is referred to the Web version of this article.)

Table 1
Radiocarbon ages and calibrated dates.

Lab. Code	Depth (cm)	Material dated	^{14}C age (a BP)	2 σ age-ranges (cal. a BP)	Midpoint calibrated age (a BP)	Midpoint age (calendar yr)
Gda-7860	23–25	Pollen	589 ± 27	646–584	612	1338 CE
Gda-7607	32–34	Pollen	2023 ± 27	2006–1882	1951	1 BCE
Gda-7608	50–52	Pollen	3944 ± 33	4447–4289	4351	2401 BCE

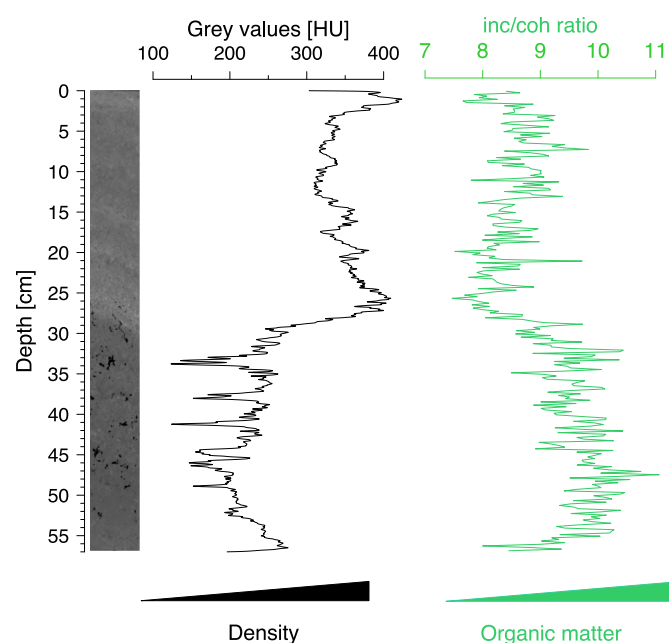


Fig. 3. CT scan image, grey values, and Inc/Coh ratio of the Lake Alchichica sediment core. The inverse correlation between the Inc/Coh ratio and grey values suggests that increased detrital input in the section above 27 cm has raised sediment density while diluting the organic matter content.

4.2. Local erosion inferred from sediment geochemistry

Eleven of the geochemical elements measured using XRF core scanning (Fe, Ti, K, Mn, Cl, Si, Zr, Ca, Sr, Cu, and Ni) demonstrate continuous abundances throughout the sediment core. We conducted a principal component analysis (PCA) on these elements to identify the primary variance patterns within the XRF dataset. The first principal component (PC1), which explains 54.3 % of the total variance, represents a gradient between siliciclastic elements (Fe, Ti, and K) on the negative axis and carbonaceous elements (Ca and Sr) on the positive axis (Fig. S1). Consequently, PC1 is interpreted as reflecting the contrast between terrigenous (allochthonous) and lacustrine (authigenic) element contributions in the lake sediments. The strong correlation ($r = 0.8$) between immobile Ti and mobile K suggests that both are derived from the same source related to the detrital flux and rules out significant post-depositional alterations in the detrital elements. Therefore, we use downcore variations in Ti, which is neither mobile nor redox-sensitive, as a proxy for detrital input into the lake, aligning with its application elsewhere in Mexico (Caballero et al., 2023; Fagel et al., 2024; Metcalfe et al., 2010; Ortega-Guerrero et al., 2021; Rantala et al., 2025; Wogau et al., 2022).

4.3. Stable isotope geochemistry as a proxy for hydroclimate conditions

In close lake systems with a seasonally dry climate, the isotopic composition of lake water is primarily controlled by the evaporation-to-precipitation (E/P) ratio (Bhattacharya et al., 2015; Covich and Stuiver, 1974; Curtis et al., 1996; Fontes and Gonfiantini, 1967; Gasse et al., 1990; Lister et al., 1991; Talbot, 1990). Elevated E/P ratios during dry conditions lead to a greater loss of lighter isotopes (^{16}O), resulting in higher

(enriched) $^{18}\text{O}/^{16}\text{O}$ ratios in both the lake water and the carbonates precipitated in equilibrium with it. In contrast, lower E/P ratios during wet conditions lead to lower (depleted) $^{18}\text{O}/^{16}\text{O}$ ratios. Given the dominance of summer rainfall in Central Mexico, driven by the monsoon,

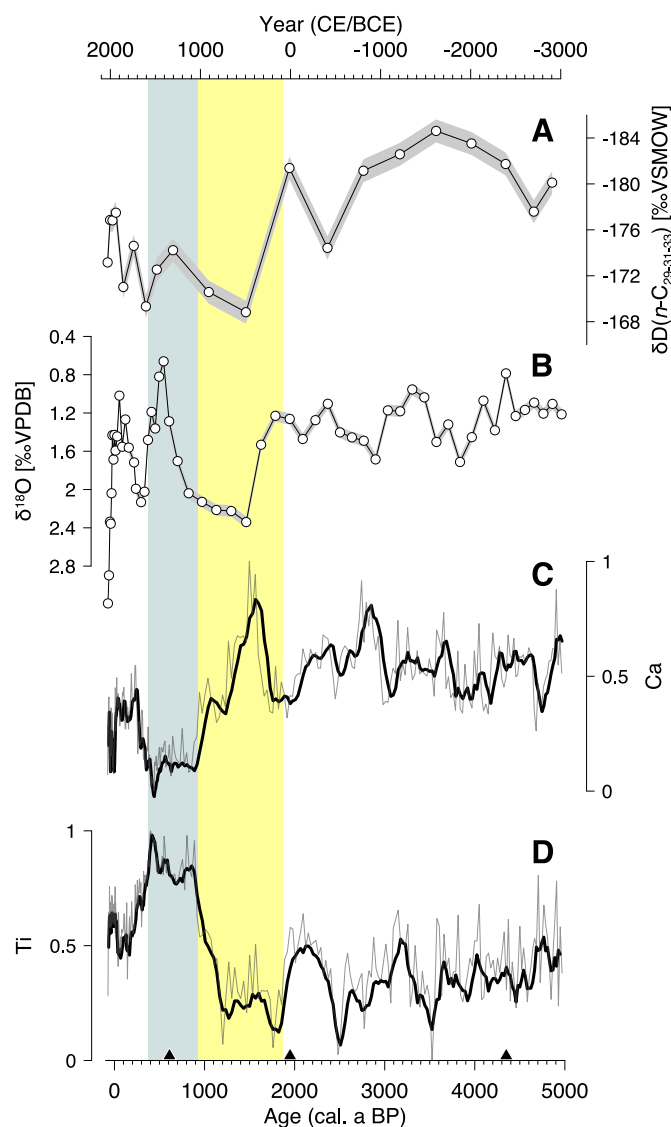


Fig. 4. Downcore variations in proxy records from the Lake Alchichica sediment core. (A) amount-weighted deuterium isotopes (δD) of n -alkane homologues derived from plant leaf waxes; (B) stable oxygen isotopes ($\delta^{18}\text{O}$) of bulk sediments. Values in A and B are reported in per mil (‰) Vienna Standard Mean Ocean Water (VSMOW) and Vienna PeeDee Belemnite (VPDB), respectively, and light grey envelopes represent analytical uncertainties. Centered log-ratio (clr) transformed and min-max normalized Ca (C) and Ti (D) intensity (grey curves) with a five-point moving average (solid black curves). Black triangles at the bottom indicate the position of ^{14}C age controls for the sediment core. Yellow and grey vertical bands highlight a shift from low (yellow) to high (grey) detrital input/erosion during the transition from the Classic to the Postclassic period. (For interpretation of the references to colour in this figure legend, the reader is referred to the Web version of this article.)

variations in $\delta^{18}\text{O}$ recorded in Lake Alchichica sediments (Fig. 4) likely reflect changes in this summer precipitation, consistent with other lacustrine records from the region (Bhattacharya et al., 2015).

Complementary evidence is provided by δD isotope data from sedimentary plant leaf wax *n*-alkanes, a proxy increasingly used in recent decades for reconstructing hydroclimate conditions (e.g., Bhattacharya et al., 2018; Contreras-Rosales et al., 2014; Douglas et al., 2015; Schefuß et al., 2005). The δD values of long-chain *n*-alkanes primarily reflect the isotopic composition of rainwater, the main moisture source for terrestrial plants, though pre-uptake evaporation can modify this signal. Notably, δD values of terrestrial plants are unaffected by non-climatic factors, such as hydrothermal inputs, which can alter water isotope compositions in crater lakes. The consistent patterns observed between δD and $\delta^{18}\text{O}$ records highlight the role of climate, particularly the E/P ratio, in shaping these isotope signals. We therefore interpret more enriched δD values as indicative of drier conditions, consistent with the amount effect, further reinforcing their climatic significance.

In Lake Alchichica sediments, δD values of homologues *n*-C₂₉, *n*-C₃₁, and *n*-C₃₃ exhibit similar patterns, implying that the same factor—rainfall—has primarily controlled the isotopic signal of these compounds. The alkane fractions are dominated by long-chain ($>\text{n-C}_{27}$) homologues typical of terrestrial plants, with negligible aquatic contributions (*n*-C₂₃, *n*-C₂₅). Low Paq values (≤ 0.21) confirm that aquatic inputs to the long-chain *n*-alkanes are minimal (Fig. S3). We therefore calculated the amount-weighted δD of *n*-C₂₉, *n*-C₃₁, and *n*-C₃₃ to capture the integrated isotopic signal of the homologous series. Furthermore, the $\delta^{13}\text{C}$ values of long-chain *n*-alkanes (C₂₉, C₃₁, C₃₃) show a marked depletion over the past few decades, likely reflecting the so-called “Suess effect” (Keeling, 1979)—a decline in atmospheric $^{13}\text{C}/^{12}\text{C}$ ratios due to the combustion of fossil fuels. Aside from this recent anthropogenic signal, $\delta^{13}\text{C}$ values remain relatively stable over the past 5000 years (Fig. S3), indicating minimal shifts in dominant plant photosynthetic pathways (e.g., C₃ vs. C₄ vegetation), therefore ruling out an influence of changing hydrogen isotope fractionation on δD values. Given this consistency and the climatic sensitivity of the isotopic records, we interpret the better-resolved $\delta^{18}\text{O}$ record as a proxy for the evaporation-to-precipitation (E/P) ratio, capturing the integrated effects of precipitation and evaporation to reconstruct past moisture variability in the region.

4.4. Palynological evidence of agricultural activity and landscape alteration

Fifty-one pollen types were identified in the Lake Alchichica

sediment core, of which 21 belong to tree taxa, 27 to herbs and shrubs, and 3 to aquatics. A pollen percentage diagram representing selected taxa is presented in Fig. 5. The CONISS clustering analysis identified two primary local pollen assemblage zones (LPAZ), labeled A and B, with zone A further subdivided into subzones A1 and A2. Overall, the dry oak forests, which dominate the present-day highlands of the Cuenca Oriental, are the predominant vegetation type throughout the record. *Pinus* (pine) pollen, the dominant pollen in the record, originates largely from temperate pine forests on the windward sides of the study area. Asteraceae and Brassicaceae plants are commonly associated with disturbed areas and agricultural fields (Jones, 1994; Li et al., 2015; Park et al., 2010; Piperno, 2006; Yang et al., 2012), which along with *Zea mays* (maize), serve as indicators of anthropogenic activity. Amaranthaceae (now encompassing formerly Amaranthaceae and Chenopodiaceae) pollen is likely linked to the growth of halophytic taxa within this family along shorelines (Regina Costa-Becheleni et al., 2021). *Glomus* spores, a type of mycorrhizal fungus, are associated with soil erosion (Anderson et al., 1984; Gelorini et al., 2011; López-Vila et al., 2014) and thus indicate local erosion dynamics.

LPAZ A1 (5000–2000 cal. a BP) represents the highest abundance of tree pollen, averaging 90 %, predominantly composed of *Pinus* (63 %), *Quercus* (17 %), *Cupressus* (4.5 %), and *Alnus* (4 %). Herbaceous pollen constitutes 10 % of the total composition, consisting of Asteraceae (3.7 %), Poaceae (3 %), and Amaranthaceae (1 %) (Fig. 5). Maize appears around 4300 cal. a BP and occurs sporadically in this zone. This pollen assemblage suggests that dry oak forests were the predominant vegetation between ca. 5000 and 2000 cal. a BP, with minimal human impact and limited agricultural activity.

LPAZ A2 (2000–1330 cal. a BP) indicates that the dominant vegetation was dry oak forests in the highlands (average tree pollen: 85 %). However, a key distinction is a decrease in *Pinus* pollen from 63 % in LPAZ A1 to 53 %, alongside an increase in Asteraceae from 3.7 % to 6.7 %. Maize occurs continuously but in low abundance (0.3 %). The presence of maize, along with Asteraceae, may indicate a slight increase in human activity between 2000 and 1330 cal. a BP.

The transition from LPAZ A to B (1330 cal. a BP to present) is characterized by significant changes in pollen composition. Tree pollen decreases to 72 %, while the proportion of herbs and shrubs increases to 28 %. *Pinus* (48 %) and *Quercus* (12 %) reach their lowest abundances in the entire record. In contrast, Asteraceae rises to 12.5 %, and Brassicaceae expands notably, comprising up to 8 % of the pollen composition. These taxa reflect a substantial increase in environmental disturbance and agricultural activities around Lake Alchichica. This pattern is

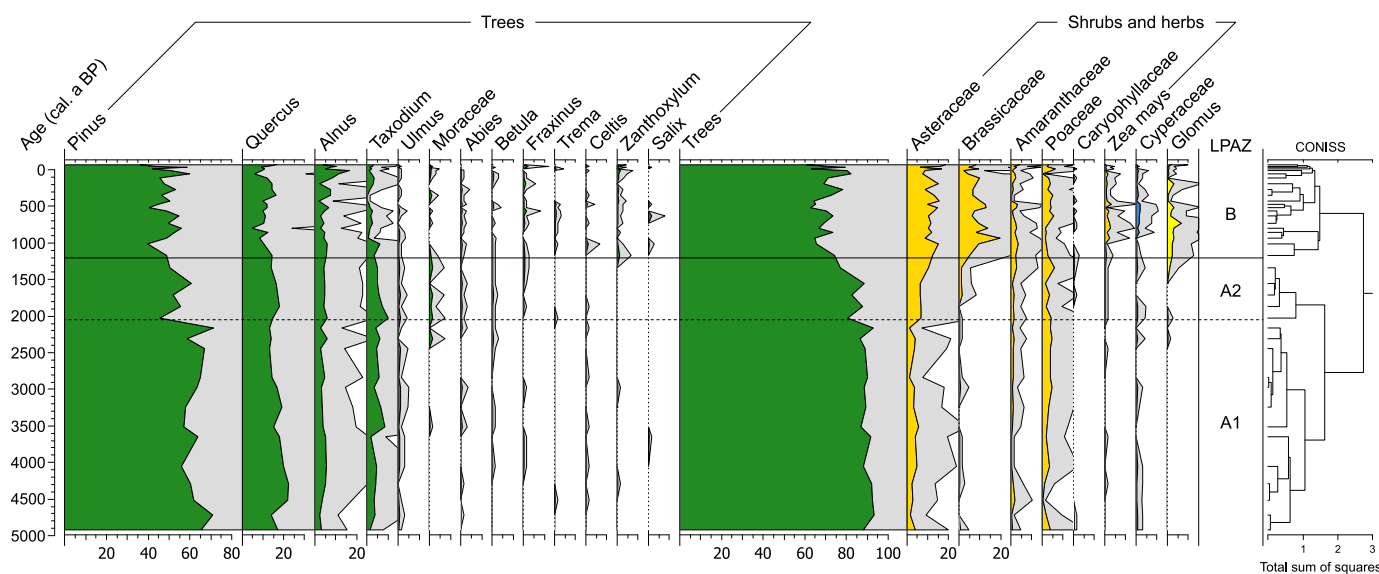


Fig. 5. Pollen percentage diagram of selected taxa from the Lake Alchichica sediment core. Local pollen assemblage zones (LPAZ) are identified through CONISS analysis (right). Grey shadings represent 5 \times exaggeration of base curves.

further supported by a significant increase in maize pollen, reaching 1.2 %, indicating a marked enhancement in farming activity. Moreover, the continued presence of *Glomus* spores suggests additional evidence of intensified erosion, which corresponds to a higher sedimentation rate. It is worth noting that, although wild maize (teosinte) also occurs in Mexico (Aguirre-Liguori et al., 2016) and produces pollen grains nearly identical to those of cultivated maize (Holst et al., 2007), the occurrence of maize pollen alongside other indicators of human activity—such as intensified soil erosion inferred from *Glomus* spores and the spread of anthropogenic plants—supports the interpretation that the maize pollen found in Lake Alchichica sediments is of domesticated origin. In addition to contextual evidence, we also used pollen size as a diagnostic criterion, since cultivated maize pollen grains are typically larger than 80 µm, which distinguishes them from their wild relatives. Another feature of LPAZ B is the increased abundance of Cyperaceae (0.1 %), which is thought to thrive along the inundated margins of the lake (Matías-Hernández and Ramírez-García, 2022). Overall, the changes in pollen composition suggest that the decline in pine and oak pollen may result from forest clearing by local communities, as also indicated by pollen records from Lake Aljojuca (Bhattacharya and Byrne, 2016). Additionally, the reduced percentages of arboreal pollen (AP) may partly reflect a dilution effect caused by an increased influx of anthropogenic pollen.

5. Discussion

5.1. Hydroclimate changes in the Cuenca Oriental

Our proxy records from Lake Alchichica provide new insights into the hydroclimatic dynamics of the Cuenca Oriental over the past 5000 years. The $\delta^{18}\text{O}$ record indicates three distinct dry periods characterized by increased E/P ratios. The first dry period occurred between approximately 500 and 1300 CE, the second during the 17th century CE, coinciding with colder temperatures during the Little Ice Age (LIA), and the third and most recent dry period began post-1970 CE. Apart from these intervals, the $\delta^{18}\text{O}$ data indicate relatively humid climatic conditions during the remaining periods (Fig. 6). It is important to note that Lake Alchichica, located in Puebla State in east-central Mexico, is primarily influenced by moisture transport from the Gulf of Mexico and the Caribbean. As a result, hydroclimate proxies from this lake, such as δD and $\delta^{18}\text{O}$, are particularly sensitive to variations in precipitation originating from the Gulf/Caribbean region rather than the Pacific. This makes the Alchichica record especially valuable for assessing hydroclimate variability driven by Atlantic-sourced moisture, in contrast to records further west that may reflect a combination of Pacific and Atlantic influences.

The interval from ca. 3000 BCE to 300 CE is characterized by moderate fluctuations in the $\delta^{18}\text{O}$ isotope data (Fig. 6) and minimal changes in vegetation composition (Fig. 5), predominantly consisting of oak forests in the highlands. This evidence suggests a lack of major hydroclimate shifts, indicating relatively wet and stable climate conditions during this time.

Beginning in the third century CE, the $\delta^{18}\text{O}$ record reveals a drying trend that culminated around 500 CE and persisted until approximately 1300 CE. This prolonged arid phase, also documented in other records from eastern Mexico, including Aljojuca, ca. 40 km southwest of Lake Alchichica (Bhattacharya et al., 2015) and Punta Laguna in the northern Yucatán (Curtis et al., 1996) (Fig. 6), represents one of the driest and longest intervals of the Holocene (Metcalfe and Davies, 2007), commonly referred to as the Late Classic Drought (Aimers, 2007; Curtis et al., 1996; Kennett et al., 2012). However, the aridity observed in Alchichica and Aljojuca extended beyond the Classic period and encompassed parts of the Postclassic period (up to ca. 1300 CE). At the beginning of the first millennium CE, an increase in Asteraceae pollen was accompanied by a decline in pine and a slight rise in oak pollen (LPAZ A2 in Fig. 5). This shift in pollen composition likely reflects a

reduction in moisture availability, which contributed to a decrease in the density of temperate pine forests on the windward slopes east of the Cuenca Oriental and facilitated the expansion of Asteraceae plants near Lake Alchichica. The low abundance of key anthropogenic indicators such as pollen of maize and Brassicaceae, and *Glomus* spores, suggests that Asteraceae proliferated in an arid rather than disturbed environment during this period. The arid conditions likely led to lower lake levels, facilitating the colonization of halophytic Amaranthaceae species on the exposed lakebed along the shorelines. The drop in lake levels also caused lake water to become saturated with carbonates, leading to the maximum precipitation of aragonite (Fig. S2) and calcium (Fig. 4). Additionally, reduced runoff activity during this arid phase significantly decreased detrital input into the lake (yellow band in Fig. 4).

The Alchichica $\delta^{18}\text{O}$ record indicates a peak in humidity around 1400 CE, a pattern also observed in Lake Aljojuca (Fig. 6) and the $\delta^{18}\text{O}$ record of a stalagmite from Juxtlahuaca Cave in Guerrero State (Lachniet et al., 2012). Following this humid phase, conditions became drier in the 17th century, partially coinciding with the Maunder Minimum (1645–1715 CE), one of the coldest intervals of the LIA. Given the low temperatures during this period, arid conditions may be attributed to reduced precipitation rather than increased evaporation.

From the mid-18th century onward, wetter conditions prevailed until the late 20th century, when $\delta^{18}\text{O}$ data reveal a trend toward their most enriched values after approximately 1970 CE. This shift may be partially attributed to a reduction in groundwater inflow due to intensive groundwater exploitation in recent decades (Alcocer et al., 2004), which has contributed to the lowering of the lake level in Alchichica (Alcalá, 2004; Alcocer and Escobar-Briones, 2007; Silva-Aguilera, 2019; Silva-Aguilera and Escolero, 2019). Overall, these findings demonstrate that the semi-arid highlands in the Cuenca Oriental are highly sensitive to cold and warm temperature anomalies and experience drier conditions during such events. Moreover, because our δD record mainly reflects precipitation variability rather than solely temperature- or evaporation-driven aridity, it provides strong evidence that major drought episodes in this region, including the Classic Drought, were in large part driven by reductions in precipitation. This represents a significant advance over previous records, which could not fully disentangle the relative roles of temperature and rainfall.

5.2. Anthropogenic changes around Lake Alchichica and their cultural implications

Evidence from the sediments of Lake Alchichica—including maize and other anthropogenic pollen, along with indicators of soil erosion such as *Glomus* spores and Ti intensity—provides valuable insights into past human–environment interactions in the region. These data indicate that continuous maize cultivation began in the middle of the first millennium BCE, corresponding to the Formative period—a pattern also observed in other sites in the Cuenca Oriental (Bhattacharya and Byrne, 2016) and central Mexico (Park et al., 2010; Watts and Bradbury, 1982).

By the early first millennium CE, a notable decline in pine forests and a concurrent rise in Asteraceae plants are evident. Species from the Asteraceae family are well adapted to arid and disturbed environments. While intensified human activity may have contributed to their spread, isotope evidence from Lake Alchichica points to increasingly dry climatic conditions, which likely facilitated their expansion. The limited presence of other anthropogenic pollen and relatively low soil erosion suggest that agricultural activity remained moderate until approximately 800 CE.

After 800 CE, the data indicate a significant intensification of human activity. This is reflected in peaks of Brassicaceae and maize pollen, alongside enhanced soil erosion, reaching a maximum during the early second millennium CE—coinciding with the transition from the Classic to the Postclassic period. Supporting this interpretation, Heine (2003) found that human activity, rather than natural factors, was the primary driver of soil erosion in the Puebla region over the past millennium.

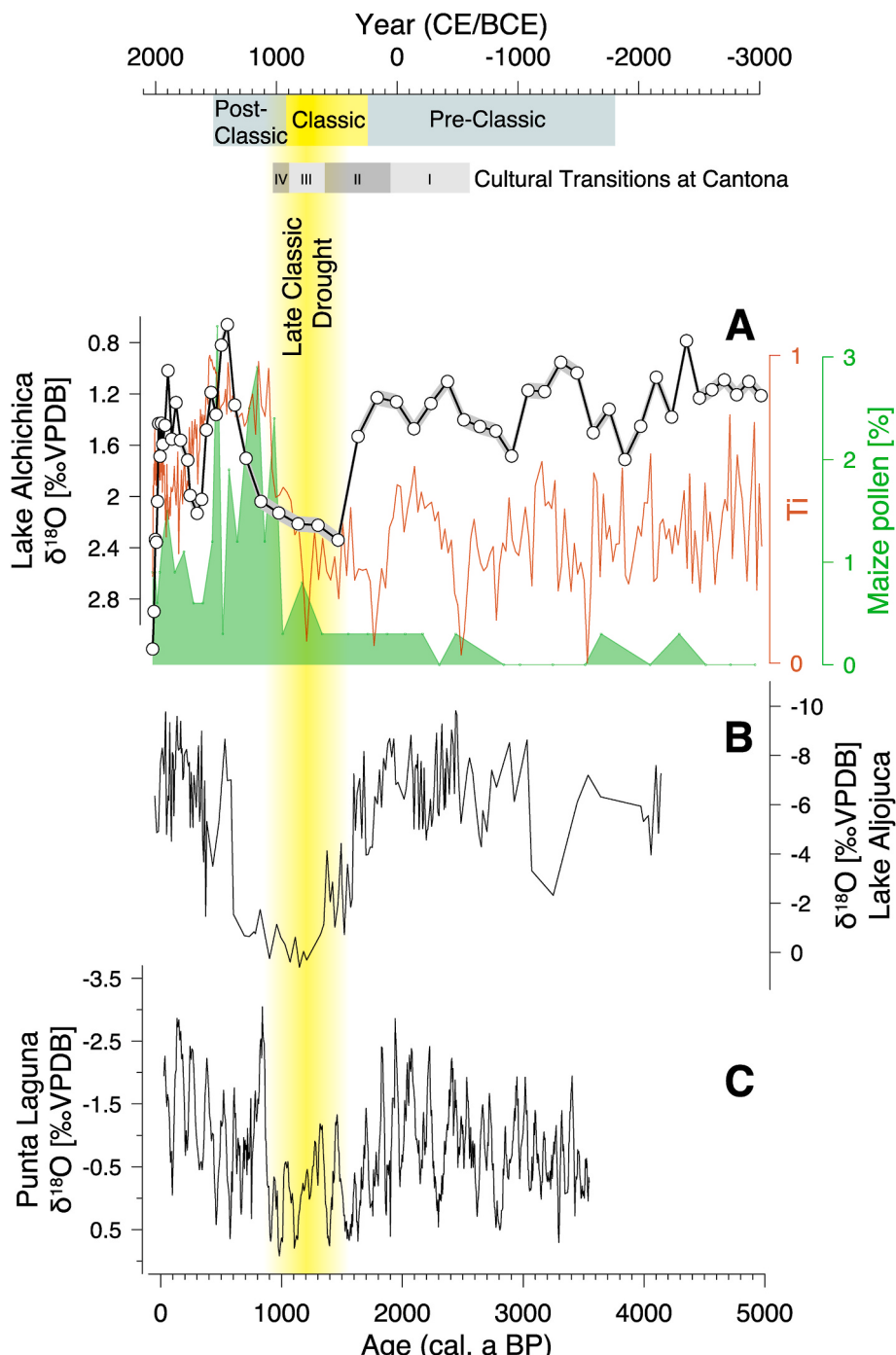


Fig. 6. Hydroclimate and anthropogenic dynamics in the Cuenca Oriental over the past 5000 years. (A) The $\delta^{18}\text{O}$ record in black (representing the E/P ratio), Ti intensity in red (indicating detrital input), and maize pollen percentages in green (reflecting maize cultivation) from the Lake Alchichica sediment core. (B) The $\delta^{18}\text{O}$ record from Lake Aljojuca (Bhattacharya et al., 2015). (C) The gastropod $\delta^{18}\text{O}$ record from Punta Laguna, northern Yucatán (Curtis et al., 1996). The Late Classic Drought (yellow band) in the Lake Alchichica $\delta^{18}\text{O}$ record aligns with shifts in the $\delta^{18}\text{O}$ records from Lake Aljojuca, but persists longer than in Punta Laguna. Mesoamerican cultural periods and transitions at Cantona (García-Cook and Merino, 1998; García Santos et al., 2012) are shown at the top. (For interpretation of the references to colour in this figure legend, the reader is referred to the Web version of this article.)

Anthropogenic indicators from Lake Alchichica suggest that between approximately 1000 and 1500 CE, corresponding to the Postclassic period, agricultural activity around Lake Alchichica reached its peak, followed by an abrupt decline with the onset of the Spanish Conquest (1521 CE). This decline was likely driven by a population collapse following the introduction of Old World diseases, to which indigenous communities lacked immunity (Cook and Simpson, 1948; Gerhard, 1972; Thomas, 1993). Consequently, agricultural activity diminished

and did not recover to the levels attained during the Postclassic period.

Our new proxy data from Lake Alchichica, combined with previously available records from Lake Aljojuca (~50 km southwest of Cantona), provide valuable insights into the climate and environmental conditions throughout the entire urban lifespan of Cantona. Both records reveal a prolonged dry interval between approximately 500 and 1300 CE, confirming that this drought affected the entire Cuenca Oriental region and that Cantona's urban period (~600–1050 CE) nested within this arid

phase. This dry interval includes the well-documented Late Classic drought (770–1100 CE) but extends beyond it, persisting longer than the dry periods observed in adjacent lowland regions such as the Gulf of Mexico (e.g., Punta Laguna; (Curtis et al., 1996); see Fig. 6). These regional hydroclimate records indicate that Cantona's collapse occurred under climate conditions comparable to those during its peak, thereby suggesting that climate was not the primary driver of the city's abandonment. Supporting this, our anthropogenic records from Lake Alchichica show a marked increase in agricultural activity beginning around 1050 CE, coinciding with Cantona's decline. This suggests that despite persistent aridity, environmental conditions remained conducive to maize cultivation. This represents one of the first lines of direct paleoenvironmental evidence for agricultural intensification in the Cuenca Oriental following the collapse of Cantona. Our findings provide empirical support for prior archaeological hypotheses that emphasized the importance of Lake Alchichica as a resource area for nearby urban centers, including Cantona (Montero-García and Junco-Sánchez, 2022), and suggest that the lake basin became a focal point for rural subsistence economies after the abandonment of the city. We propose that following the collapse of urban system of Cantona, a rural lifestyle based on intensified maize agriculture developed in the Lake Alchichica area. Taken together, the regional climate conditions inferred from proxy records from Lake Alchichica and Aljojuca suggest that climate stress alone was insufficient to cause the abandonment of the city. We therefore propose that non-climatic factors, such as warfare, socio-political instability, and economic disruption, also played significant roles in the abandonment of Cantona. However, further archaeological evidence will be necessary to pin down the primary causes of its abandonment.

6. Conclusions

The proxy records from the Lake Alchichica sediment core provide independent evidence of hydroclimate, agricultural, and anthropogenic dynamics in the Cuenca Oriental over the past five millennia. Isotope data reveal three distinct dry periods marked by elevated E/P ratios: between ~500 and 1300 CE (spanning the middle Classic to early Postclassic period), the 17th century CE (coincident with colder temperatures during the LIA), and post-1970 CE. Outside these intervals, conditions were generally more humid. Anthropogenic indicators—including maize and other anthropogenic pollen, and soil erosion inferred from *Glomus* spores and Ti intensity—demonstrate long-term human–environment interactions. Continuous maize cultivation began by the mid-first millennium BCE, with moderate agricultural activity persisting until around 800 CE. A marked intensification of agriculture occurred during the Postclassic period (ca. 1000–1500 CE), evidenced by peaks in maize and Brassicaceae pollen and increased soil erosion, followed by a sharp decline after the Spanish Conquest in 1521 CE, likely due to demographic collapse from introduced diseases.

These findings provide new insights into the environmental context in which the urban system of Cantona emerged and eventually declined. A prolonged dry period from ca. 500 to 1300 CE encompassed the entirety of urban era of Cantona (600–1050 CE). We show that the decline of Cantona between ca. 900 and 1050 CE occurred under hydroclimatic conditions comparable to those during its peak. Crucially, a sharp increase in agricultural activity around Lake Alchichica coincided with the abandonment of Cantona suggests that aridity alone does not fully explain the abandonment and pointing to additional factors such as warfare, socio-political instability, or economic disruption.

Author contributions

Reza Safaierad: Writing – original draft, Visualization, Validation, Software, Project administration, Investigation, Formal analysis, Data curation, Conceptualization., **Isabel Israde-Alcántara:** Writing – review & editing, Validation, Resources, Funding acquisition, Conceptualization., **Marttiina Rantala:** Writing – review & editing, Validation,

Investigation, Data curation, Conceptualization. **Gabriela Domínguez-Vázquez:** Writing – review & editing, Formal analysis., **Mahyar Mohattadi:** Writing – review & editing, Resources, Validation, Formal analysis., **Enno Schefuß:** Writing – review & editing, Resources, Validation, Formal analysis., **Wojciech Tylmann:** Writing – review & editing, Validation, Resources, Formal analysis., **Pierre Francus:** Writing – review & editing, Resources, Formal analysis., **Nadine Mattielli:** Writing – review & editing, Project administration, Conceptualization., **Sarah Metcalfe:** Writing – review & editing, Investigation., **Nathalie Fagel:** Writing – review & editing, Resources, Project administration, Investigation, Funding acquisition, Conceptualization.

Declaration of competing interest

All authors declare that there are no competing interests.

Acknowledgments

This research was funded by the Fonds National de la Recherche Scientifique (F.R.S.-FNRS) as part of the *HolMeCl: Holocene Mexican Crater Lakes and Climate* project. Isabel Israde-Alcántara acknowledges support by Instituto de Investigaciones en Ciencias de la Tierra (ICTI-PICIR23-01). We thank Joël Otten (University of Liege), Henning Kuhnert, Birgit Meyer-Schack and Ralph Kreutz (MARUM) for their technical support. We appreciate the assistance of Valentine Piroton, Julio Cañas and Luis Matilde Garcia during fieldwork and the sediment core collection. We also thank the handling editor and the reviewers, including Dr. Tripti Bhattacharya and one anonymous reviewer, for their thoughtful comments and suggestions.

Appendix A. Supplementary data

Supplementary data to this article can be found online at <https://doi.org/10.1016/j.quascirev.2025.109618>.

Data availability

All of the data that support the findings of this paper have been deposited in PANGAEA (PDI-40779).

References

- Adams, D.K., Comrie, A.C., 1997. The North American monsoon. *Bull. Am. Meteorol. Soc.* 78, 2197–2214.
- Aguirre-Liguori, J.A., Aguirre-Planter, E., Eguiarte, L.E., 2016. Genetics and ecology of wild and cultivated maize: domestication and introgression. In: Lira, R., Casas, A.J.B. (Eds.), *Ethnobotany of Mexico: Interactions of People and Plants in Mesoamerica*. Springer, New York, pp. 403–416.
- Aimers, J.J., 2007. What Maya collapse? Terminal Classic variation in the Maya lowlands. *J. Archaeol. Res.* 15, 329–377. <https://doi.org/10.1007/978-1-4614-6669-7>.
- Alcalá, A., 2004. *Estudio hidrogeológico de Alchichica, estado de Puebla*. Bachelor Thesis. Universidad Nacional Autónoma de México, México.
- Alcocer, D., Escalero, F., Marín, L., 2004. Problemática del agua de la Cuenca Oriental, estados de Puebla, Veracruz y Tlaxcala. In: Mazari-Hiriart, M., Lesser, J.M. (Eds.), *El Agua en México vista desde la Academia*. Academia Mexicana de Ciencias, México, pp. 57–77.
- Alcocer, J., Escobar-Briones, E., 2007. On the ecology of *Caecidotea williamsi* Escobar-Briones & Alcocer (Crustacea: Isopoda: Asellidae) from Alchichica saline lake, Central Mexico. *Hydrobiologia* 576, 103–109. <https://doi.org/10.1007/s10750-006-0297-7>.
- Almeida-Leñero, L., Hooghiemstra, H., Cleef, A.M., van Geel, B., 2005. Holocene climatic and environmental change from pollen records of lakes Zempoala and Quila, central Mexican highlands. *Rev. Palaeobot. Palynol.* 136, 63–92. <https://doi.org/10.1016/j.revpalbo.2005.05.001>.
- Anderson, R.S., Homola, R.L., Davis, R.B., Jacobson Jr, G.L., 1984. Fossil remains of the mycorrhizal fungal *Glomus fasciculatum* complex in postglacial lake sediments from Maine. *Can. J. Bot.* 62, 2325–2328. <https://doi.org/10.1139/b84-316>.
- Aquino-López, M.A., Blaauw, M., Christen, J.A., Sanderson, N.K., 2018. Bayesian analysis of 210 Pb dating. *J. Agric. Biol. Environ. Stat.* 23, 317–333. <https://doi.org/10.1214/10-BA60>.

- Arnauld, C., Metcalfe, S.E., Petrequin, P., 1997. Holocene climatic change in the Zacapu lake basin, Michoacan: synthesis of results. *Quat. Int.* 43, 173–179. [https://doi.org/10.1016/S1040-6182\(97\)00033-5](https://doi.org/10.1016/S1040-6182(97)00033-5).
- Arredondo-Figueroa, J.L., Borrego-Enríquez, L., Castillo-Domínguez, R., Valladolid-Laredo, M., 1983. Batimetría y morfometría de los lagos 'maars' de la cuenca de Oriental, Puebla. *Méjico. Biótica* 8, 37–47.
- Bhattacharya, T., Byrne, R., 2016. Late Holocene anthropogenic and climatic influences on the regional vegetation of Mexico's Cuenca Oriental. *Global Planet. Change* 138, 56–69. <https://doi.org/10.1016/j.gloplacha.2015.12.005>.
- Bhattacharya, T., Byrne, R., Böhnel, H., Wogau, K., Kienel, U., Ingram, B.L., Zimmerman, S., 2015. Cultural implications of late Holocene climate change in the Cuenca Oriental, Mexico. *Proc. Natl. Acad. Sci.* 112, 1693–1698. <https://doi.org/10.1073/pnas.1405653112>.
- Bhattacharya, T., Tierney, J.E., Addison, J.A., Murray, J.W., 2018. Ice-sheet modulation of deglacial North American monsoon intensification. *Nat. Geosci.* 11, 848–852. <https://doi.org/10.1038/s41561-018-0220-7>.
- Brenner, M., Rosenmeier, M.F., Hodell, D.A., Curtis, J.H., 2002. Paleolimnology of the Maya lowlands: long-term perspectives on interactions among climate, environment, and humans. *Anc. Mesoam.* 13, 141–157. [10.1017/S0956536102131063](https://doi.org/10.1017/S0956536102131063).
- Butzer, K.W., Butzer, E.K., 1997. The 'natural' vegetation of the Mexican Bajío: Archival documentation of a 16th-century savanna environment. *Quat. Int.* 43, 161–172. [https://doi.org/10.1016/S1040-6182\(97\)00032-3](https://doi.org/10.1016/S1040-6182(97)00032-3).
- Caballero, M., Lozano-García, S., Romero, M.V., Sosa, S., 2023. Droughts during the last 2000 years in a tropical sub-humid environment in central Mexico. *J. Quat. Sci.* 38, 767–775. <https://doi.org/10.1002/jqs.3509>.
- Caballero, M., Vilalcará, G., Rodríguez, A., Juárez, D., 2003. Short-term climatic change in lake sediments from lake Alchichica, Oriental, Mexico. *Geofis. Int.* 42, 529–537. <https://doi.org/10.22201/igeof.00167169p.2003.42.3.942>.
- Colorado-Ruiz, G., Cavazos, T., Salinas, J.A., De Grau, P., Ayala, R., 2018. Climate change projections from Coupled Model Intercomparison Project phase 5 multi-model weighted ensembles for Mexico, the North American monsoon, and the mid-summer drought region. *Int. J. Climatol.* 38, 5699–5716. <https://doi.org/10.1002/joc.5773>.
- Conterras-Rosas, L.A., Jennerjahn, T., Tharammal, T., Meyer, V., Lückge, A., Paul, A., Schefuß, E., 2014. Evolution of the Indian Summer Monsoon and terrestrial vegetation in the Bengal region during the past 18 ka. *Quat. Sci. Rev.* 102, 133–148. <https://doi.org/10.1016/j.quascirev.2014.08.010>.
- Cook, S.F., Simpson, L.B., 1948. *The Population of Central Mexico in the Sixteenth Century*. University of California Press, Berkeley.
- Covich, A., Stuiver, M., 1974. Changes in oxygen 18 as a measure of long-term fluctuations in tropical lake levels and molluscan populations 1. *Limnol. Oceanogr.* 19, 682–691. <https://doi.org/10.4319/lo.1974.19.4.0682>.
- Curtis, J.H., Hodell, D.A., Brenner, M., 1996. Climate variability on the Yucatan Peninsula (Mexico) during the past 3500 years, and implications for Maya cultural evolution. *Quat. Res.* 46, 37–47. <https://doi.org/10.1006/qres.1996.0042>.
- Douglas, P.M., Paganí, M., Canuto, M.A., Brenner, M., Hodell, D.A., Eglington, T.I., Curtis, J.H., 2015. Drought, agricultural adaptation, and sociopolitical collapse in the Maya Lowlands. *Proc. Natl. Acad. Sci.* 112, 5607–5612. <https://doi.org/10.1073/pnas.1419133112>.
- Elliott, M., Fisher, C.T., Nelson, B.A., Garza, R.S.M., Collins, S.K., Pearsall, D.M., 2010. Climate, agriculture, and cycles of human occupation over the last 4000 yr in southern Zacatecas, Mexico. *Quat. Res.* 74, 26–35. <https://doi.org/10.1016/j.yqres.2010.04.001>.
- Ernesto Rivera-Hernandez, J., Flores-Hernandez, N., Felipe Vargas-Rueda, A., Alcantara-Salinas, G., de Jesus Chazarro-Basanez, M., Cruz Garcia-Albarado, J., 2019. Flora and vegetation from the semiarid region of Acultzingo-Maltrata, Veracruz, Mexico. *Acta Bot. Mex.* 126, e1433. <https://doi.org/10.21829/abm126.2019.1433>.
- Estrada-Belli, F., Wahl, D., 2010. Prehistoric Human-Environment Interactions in the Southern Maya Lowlands: the Holmul Region Case. Final report to the National Science Foundation. <http://www.bu.edu/holmul>.
- Faegri, K., Iversen, J., 1989. In: Faegri, K., Kaland, P.E., Krzywinski, K. (Eds.), *Textbook of Pollen Analysis*, fourth ed. Wiley, New York.
- Fagel, N., Israde-Alcántara, I., Safaierad, R., Rantala, M., Schmidt, S., Leپoint, G., Pellenard, P., Mattielli, N., Metcalfe, S., 2024. Environmental significance of kaolinite variability over the last centuries in crater lake sediments from Central Mexico. *Appl. Clay Sci.* 247, 107211. <https://doi.org/10.1016/j.clay.2023.107211>.
- Ficken, K.J., Li, B., Swain, D., Eglington, G., 2000. An n-alkane proxy for the sedimentary input of submerged/floating freshwater aquatic macrophytes. *Org. Geochem.* 31, 745–749. [https://doi.org/10.1016/S0146-6380\(00\)00081-4](https://doi.org/10.1016/S0146-6380(00)00081-4).
- Fisher, C.T., 2005. Demographic and landscape change in the Lake Pátzcuaro basin, Mexico: abandoning the garden. *Am. Anthropol.* 107, 87–95. <https://doi.org/10.1525/aa.2005.107.1.087>.
- Fontes, J.-C., Gonfiantini, R., 1967. Comportement isotopique au cours de l'évaporation de deux bassins sahariens. *Earth Planet. Sci. Lett.* 3, 258–266. [https://doi.org/10.1016/0012-821X\(67\)90046-5](https://doi.org/10.1016/0012-821X(67)90046-5).
- García-Cook, A., Merino, C.B., 1998. *Cantona: Urbe Prehispánica en el Altiplano Central de México. Latin America Antique* 9, 191–216.
- García Santos, A., Neila González, F.J., Oliver Ramírez, A., 2012. Clasificación y selección de materiales de cambio de fase según sus características para su aplicación en sistemas de almacenamiento de energía térmica. *Mater. Construcción* 62, 131–140. <https://doi.org/10.3989/mc.2012.58010>.
- Gasse, F., Téhet, R., Durand, A., Gibert, E., Fontes, J.-C., 1990. The arid–humid transition in the Sahara and the Sahel during the last deglaciation. *Nature* 346, 141–146. <https://doi.org/10.1038/346141a0>.
- Gelorini, V., Verbeken, A., van Geel, B., Cocquyt, C., Verschuren, D., 2011. Modern non-pollen palynomorphs from East African lake sediments. *Rev. Palaeobot. Palynol.* 164, 143–173. <https://doi.org/10.1016/j.revpalbo.2010.12.002>.
- Gerez-Fernández, P., 1985. *Uso del suelo durante cuatrocientos años y cambio fisionómico en la zona semiárida Poblano-Veracruzana, México*. *Biotica (Mex.)* 10, 123–144.
- Gerhard, P., 1972. *A Guide to the Historical Geography of New Spain*. Cambridge University Press, London.
- Goman, M., Joyce, A., Mueller, R., Paschyn, L., 2010. Multiproxy paleoecological reconstruction of prehistoric land-use history in the western region of the lower Rio Verde Valley, Oaxaca, Mexico. *Holocene* 20, 761–772. <https://doi.org/10.1177/0959683610362811>.
- Grimm, E.C., 1987. CONISS: a FORTRAN 77 program for stratigraphically constrained cluster analysis by the method of incremental sum of squares. *Comput. Geosci.* 13, 13–35. [https://doi.org/10.1016/0098-3004\(87\)90022-7](https://doi.org/10.1016/0098-3004(87)90022-7).
- Grimm, E.C., 1991. *TILIA and TILIA GRAPH Computer Programs*. Illinois State Museum, Springfield.
- Haug, G.H., Gunther, D., Peterson, L.C., Sigman, D.M., Hughen, K.A., Aeschlimann, B., 2003. Climate and the collapse of Maya civilization. *Science* 299, 1731–1735. <https://doi.org/10.1126/science.1080444>.
- Heine, K., 2003. Paleopedological evidence of human-induced environmental change in the Puebla-Tlaxcala area (Mexico) during the last 3,500 years. *Rev. Mex. Ciencias Geol.* 20, 235–244.
- Higgins, R., Yao, Y., Wang, X., 1997. Influence of the North American monsoon system on the US summer precipitation regime. *J. Clim.* 10, 2600–2622. [https://doi.org/10.1175/1520-0442\(1997\)010<2600:IOTNAM>2.0.CO;2](https://doi.org/10.1175/1520-0442(1997)010<2600:IOTNAM>2.0.CO;2).
- Hodell, D.A., Curtis, J.H., Brenner, M., 1995. Possible role of climate in the collapse of Classic Maya civilization. *Nature* 375, 391–394. <https://doi.org/10.1038/375391a0>.
- Holst, I., Moreno, J.E., Piperno, D.R., 2007. Identification of teosinte, maize, and Tripsacum in Mesoamerica by using pollen, starch grains, and phytoliths. *Proc. Natl. Acad. Sci.* 104, 17608–17613. <https://doi.org/10.1073/pnas.0708736104>.
- Jones, J.G., 1994. Pollen evidence for early settlement and agriculture in northern Belize. *Palynology* 18, 205–211. <https://doi.org/10.1080/01916122.1994.9989445>.
- Jull, A.T., Burr, G.S., Hodgins, G.W., 2013. Radiocarbon dating, reservoir effects, and calibration. *Quat. Int.* 299, 64–71. <https://doi.org/10.1016/j.quaint.2012.10.028>.
- Kaźmierczak, J., Kempe, S., Kremer, B., López-García, P., Moreira, D., Tavera, R., 2011. Hydrochemistry and microbialites of the alkaline crater lake Alchichica, Mexico. *Facies* 57, 543–570. <https://doi.org/10.1007/s10347-010-0255-8>.
- Keeling, C.D., 1979. The Suess effect: ¹³Carbon-¹⁴Carbon interrelations. *Environ. Int.* 2, 229–300. [https://doi.org/10.1016/0160-4120\(79\)90005-9](https://doi.org/10.1016/0160-4120(79)90005-9).
- Kennett, D.J., Breitenbach, S.F., Aquino, V.V., Asmerom, Y., Awe, J., Baldini, J.U., Bartlein, P., Culleton, B.J., Ebert, C., Jazwa, C., 2012. Development and disintegration of Maya political systems in response to climate change. *Science* 338, 788–791. <https://doi.org/10.1126/science.1226299>.
- Knight, C.L., Glascock, M.D., 2009. The terminal formative to Classic period obsidian assemblage at Palo Errado, Veracruz, Mexico. *Lat. Am. Antiq.* 20, 507–524. <https://doi.org/10.1017/S104566350002856>.
- Knutti, R., Sedláček, J., 2013. Robustness and uncertainties in the new CMIP5 climate model projections. *Nat. Clim. Change* 3, 369–373. <https://doi.org/10.1038/nclimate1716>.
- Lachniet, M.S., Bernal, J.P., Asmerom, Y., Polyak, V., Piperno, D., 2012. A 2400 yr Mesoamerican rainfall reconstruction links climate and cultural change. *Geology* 40, 259–262. <https://doi.org/10.1130/g32471.1>.
- Leyden, B.W., 1987. Man and climate in the Maya lowlands. *Quat. Res.* 28, 407–414.
- Li, M., Xu, Q., Zhang, S., Li, Y., Ding, W., Li, J., 2015. Indicator pollen taxa of human-induced and natural vegetation in Northern China. *Holocene* 25, 686–701. <https://doi.org/10.1177/095968361456621>.
- Lister, G.S., Kelts, K., Zao, C.K., Yu, J.-Q., Niessen, F., 1991. Lake Qinghai, China: closed-basin like levels and the oxygen isotope record for ostracoda since the latest Pleistocene. *Palaeogeogr. Palaeoclimatol. Palaeoecol.* 84, 141–162. [https://doi.org/10.1016/0031-0182\(91\)90041-O](https://doi.org/10.1016/0031-0182(91)90041-O).
- López-Vila, J., Montoya, E., Cañellas-Boltà, N., Rull, V., 2014. Modern non-pollen palynomorphs sedimentation along an elevational gradient in the south-central Pyrenees (southwestern Europe) as a tool for Holocene paleoecological reconstruction. *Holocene* 24, 327–345. <https://doi.org/10.1177/0959683613518>.
- Magaña, V., Amador, J.A., Medina, S., 1999. The midsummer drought over Mexico and Central America. *J. Clim.* 12, 1577–1588. [https://doi.org/10.1175/1520-0442\(1999\)012<1577:TMDDOMA>2.0.CO;2](https://doi.org/10.1175/1520-0442(1999)012<1577:TMDDOMA>2.0.CO;2).
- Matías-Hernández, E., Ramírez-García, P., 2022. Aquatic vegetation. In: Alcocer, J. (Ed.), *Lake Alchichica Limnology: the Uniqueness of a Tropical Maar Lake*. Springer, Cham, pp. 149–162. https://doi.org/10.1007/978-3-030-79096-7_9.
- Matsuoka, Y., Vigouroux, Y., Goodman, M.M., Sanchez, G.J., Buckler, E., Doebley, J., 2002. A single domestication for maize shown by multilocus microsatellite genotyping. *Proc. Natl. Acad. Sci.* 99, 6080–6084. <https://doi.org/10.1073/pnas.021521599>.
- Metcalfe, S., Davies, S., 2007. Deciphering recent climate change in central Mexican lake records. *Clim. Change* 83, 169–186. <https://doi.org/10.1007/s10584-006-9152-0>.
- Metcalfe, S.E., Jones, M.D., Davies, S.J., Noren, A., MacKenzie, A., 2010. Climate variability over the last two millennia in the North American Monsoon region, recorded in laminated lake sediments from Laguna de Juanacatlán, Mexico. *Holocene* 20, 1195–1206. <https://doi.org/10.1177/095968361037199>.
- Metcalfe, S.E., Street-Perrott, F.A., Brown, R.B., Hales, P.E., Perrott, R.A., Steininger, F.M., 1989. Late Holocene human impact on lake basins in Central Mexico. *Geoarchaeology* 4, 119–141. <https://doi.org/10.1002/gea.3340040203>.
- Montero-García, I.A., Junco-Sánchez, R.E., 2022. Lake Alchichica: history of human settlements. In: Alcocer, J. (Ed.), *Lake Alchichica Limnology: the Uniqueness of a*

- Tropical Maar Lake. Springer, Cham, pp. 1–13. https://doi.org/10.1007/978-3-030-79096-7_1.
- Moore, D.M., Reynolds Jr., R., 1989. X-Ray Diffraction and the Identification and Analysis of Clay Minerals. Oxford University Press, Oxford.
- Ortega-Guerrero, B., Caballero, M., Israde-Alcántara, I., 2021. The Holocene record of Alberca de Tacámbaro, a tropical lake in western Mexico: evidence of orbital and millennial-scale climatic variability. *J. Quat. Sci.* 36, 649–663. <https://doi.org/10.1002/jqs.3316>.
- Park, J., Byrne, R., Böhnel, H., Garza, R.M., Conserva, M., 2010. Holocene climate change and human impact, central Mexico: a record based on maar lake pollen and sediment chemistry. *Quat. Sci. Rev.* 29, 618–632. <https://doi.org/10.1016/j.quascirev.2009.10.017>.
- Piperno, D.R., 2006. Quaternary environmental history and agricultural impact on vegetation in Central America. *Ann. Mo. Bot. Gard.* 93 (2), 274–296. [https://doi.org/10.3417/0026-6493\(2006\)93\[274:QEHAJ\]2.0.CO;2](https://doi.org/10.3417/0026-6493(2006)93[274:QEHAJ]2.0.CO;2).
- Piperno, D.R., Flannery, K.V., 2001. The earliest archaeological maize (*Zea mays* L.) from highland Mexico: new accelerator mass spectrometry dates and their implications. *Proc. Natl. Acad. Sci.* 98, 2101–2103. <https://doi.org/10.1073/pnas.98.4.2101>.
- Rantala, M., Israde-Alcántara, I., Safaierad, R., Tylmann, W., Lepoint, G., Francus, P., Smol, J.P., Meyer-Jacob, C., Grooms, C., Mattielli, N., Metcalfe, S., Etmański, P., Fagel, N., 2025. Anthropogenic increase in organic carbon production and burial in two tropical Mexican crater lakes. *Sci. Total Environ.* 971, 179041. <https://doi.org/10.1016/j.scitotenv.2025.179041>.
- Regina Costa-Becheleni, F., Troyo-Dieguez, E., Nieto-Garibay, A., Alejandro Bustamante-Salazar, L., Sergio García-Galindo, H., Murillo-Amador, B., 2021. Hydro-environmental criteria for introducing an edible Halophyte from a rainy region to an arid zone: a study case of *Suaeda* spp. as a new crop in NW Mexico. *Plants* 10, 1996. <https://doi.org/10.3390/plants10101996>.
- Reimer, P.J., Austin, W.E., Bard, E., Bayliss, A., Blackwell, P.G., Ramsey, C.B., Butzin, M., Cheng, H., Edwards, R.L., Friedrich, M., 2020. The IntCal20 Northern Hemisphere radiocarbon age calibration curve (0–55 cal kBP). *Radiocarbon* 62, 725–757. <https://doi.org/10.1017/RDC.2020.41>.
- Rietveld, H., 1967. Line profiles of neutron powder-diffraction peaks for structure refinement. *Acta Crystallogr.* 22, 151–152. <https://doi.org/10.1107/s0365110x67000234>.
- Sachse, D., Billault, I., Bowen, G.J., Chikaraishi, Y., Dawson, T.E., Feakins, S.J., Freeman, K.H., Magill, C.R., McInerney, F.A., Van Der Meer, M.T., 2012. Molecular paleohydrology: interpreting the hydrogen-isotopic composition of lipid biomarkers from photosynthesizing organisms. *Annu. Rev. Earth Planet Sci.* 40, 221–249. <https://doi.org/10.1146/annurev-earth-042711-105535>.
- Scheufel, E., Schouten, S., Schneider, R.R., 2005. Climatic controls on central African hydrology during the past 20,000 years. *Nature* 437, 1003–1006. <https://doi.org/10.1038/nature03945>.
- Silva-Aguilera, R., 2019. Análisis del descenso del nivel de agua del Lago Alchichica, Puebla, México (Tesis de Maestría). Universidad Nacional Autónoma de México, Coordinación General de Estudios de Posgrado, UNAM.
- Silva-Aguilera, R., Escolero, O., 2019. El agua subterránea y el lago. Lago Alchichica: Una joya de biodiversidad. 1a edición. Facultad de Estudios Superiores Iztacala, Universidad Nacional Autónoma de México. Comisión Nacional para el Conocimiento y Uso de la Biodiversidad 49–59. Mexico City.
- Silva-Aguilera, R.A., Escolero, O., Alcocer, J., Morales-Casique, E., Olea-Olea, S., Vilalcarra, G., Lozano-García, S., Correa-Metrio, A., 2025. Climate and anthropic agents lead to changes in groundwater-surface water interactions in a semi-arid maar lake. *J. S. Am. Earth Sci.* 156, 105398. <https://doi.org/10.1016/j.james.2025.105398>.
- Simpson, L.B., 1952. Exploitation of Land in Central Mexico in the Sixteenth Century. University of California Press, Berkeley.
- Środoń, J., 2002. Quantitative mineralogy of sedimentary rocks with emphasis on clays and with applications to K-Ar dating. *Mineral. Mag.* 66, 677–687. <https://doi.org/10.1108/0026461026650055>.
- Stuiver, M., Östlund, H., 1983. GEOSECS Indian ocean and Mediterranean radiocarbon. *Radiocarbon* 25, 1–29. <https://doi.org/10.1017/S0033822200005270>.
- Talbot, M., 1990. A review of the palaeohydrological interpretation of carbon and oxygen isotopic ratios in primary lacustrine carbonates. *Chem. Geol. Isot. Geosci.* 80, 261–279. [https://doi.org/10.1016/0168-9622\(90\)90009-2](https://doi.org/10.1016/0168-9622(90)90009-2).
- Tavera, R., Komárek, J., 1996. Cyanoprokaryotes in the volcanic lake of Alchichica, Puebla State, Mexico. *Archiv für Hydrobiologie. Supplementband, Algological studies* 117, 511–538. https://doi.org/10.1127/algol_stud/83/1996/511.
- Team, R.C., 2020. RA language and environment for statistical computing. R Foundation for Statistical Computing.
- Thomas, H., 1993. Conquest: Montezuma, Cortés, and the Fall of Old Mexico. Simon & Schuster, New York.
- Tunno, I., Zimmerman, S.R., Brown, T.A., Hassel, C.A., 2021. An improved method for extracting, sorting, and AMS dating of pollen concentrates from lake sediment. *Front. Ecol. Evol.* 9, 668676. <https://doi.org/10.3389/fevo.2021.668676>.
- Turner, B.L., Sabloff, J.A., 2012. Classic Period collapse of the central Maya lowlands: insights about human-environment relationships for sustainability. *Proc. Natl. Acad. Sci.* 109, 13908–13914. <https://doi.org/10.1073/pnas.1210106109>.
- Tylmann, W., Bonk, A., Goslar, T., Wulf, S., Grosjean, M., 2016. Calibrating ^{210}Pb dating results with varve chronology and independent chronostratigraphic markers: problems and implications. *Quat. Geochronol.* 32, 1–10. <https://doi.org/10.1016/j.quageo.2015.11.004>.
- Vázquez, G., Ortega, B., Davies, S.J., Aston, B.J., 2010. Registro sedimentario de los últimos ca. 17000 años del lago de Zirahuén, Michoacán, México. *Bol. Soc. Geol. Mex.* 62, 325–343. <https://dx.doi.org/10.18268/BSGM2010v62n3a2>.
- Wahl, D., Estrada-Belli, F., Anderson, L., 2013. A 3400 year paleolimnological record of prehispanic human-environment interactions in the Holmul region of the southern Maya lowlands. *Palaeogeogr. Palaeoclimatol. Palaeoecol.* 379, 17–31. <https://doi.org/10.1016/j.palaeo.2013.03.006>.
- Walsh, M.K., Pruffer, K.M., Culleton, B.J., Kennett, D.J., 2014. A late Holocene paleoenvironmental reconstruction from Agua Caliente, southern Belize, linked to regional climate variability and cultural change at the Maya polity of Uxbenká. *Quat. Res.* 82, 38–50. <https://doi.org/10.1016/j.yqres.2014.01.013>.
- Watts, W.A., Bradbury, J.P., 1982. Paleoecological studies at lake Patzcuaro on the west-central Mexican plateau and at Chalcón in the basin of Mexico. *Quat. Res.* 17, 56–70. [https://doi.org/10.1016/0033-5894\(82\)90045-X](https://doi.org/10.1016/0033-5894(82)90045-X).
- Weltje, G.J., Bloemsma, M., Tjallingii, R., Heslop, D., Röhl, U., Croudace, I.W., 2015. Prediction of geochemical composition from XRF core scanner data: a new multivariate approach including automatic selection of calibration samples and quantification of uncertainties. In: Croudace, I., Rothwell, R. (Eds.), Micro-XRF Studies of Sediment Cores: Applications of a Non-destructive Tool for the Environmental Sciences, Developments in Paleoenvironmental Research, vol. 17. Springer, Dordrecht. https://doi.org/10.1007/978-94-017-9849-5_21.
- Wogau, K.H., Hoelzmann, P., Arz, H.W., Böhnel, H.N., 2022. Paleoenvironmental conditions during the medieval climatic anomaly, the Little Ice age and social impacts in the oriental mesoamerican region. *Quat. Sci. Rev.* 289, 107616. <https://doi.org/10.1016/j.quascirev.2022.107616>.
- Woodward, C., Gadd, P., 2019. The potential power and pitfalls of using the X-ray fluorescence molybdenum incoherent coherent scattering ratio as a proxy for sediment organic content. *Quat. Int.* 514, 30–43. <https://doi.org/10.1016/j.quaint.2018.11.031>.
- Yang, S., Zheng, Z., Huang, K., Zong, Y., Wang, J., Xu, Q., Rolett, B.V., Li, J., 2012. Modern pollen assemblages from cultivated rice fields and rice pollen morphology: application to a study of ancient land use and agriculture in the Pearl River Delta, China. *Holocene* 22, 1393–1404. <https://doi.org/10.1177/0959683612449761>.